A Combinatorial TIR1/AFB-Aux/IAA Co-receptor System for Differential Sensing of Auxin

Luz Irina A. Calderón Villalobos, Sarah Lee, Cesar De Oliveira, Anthony Ivetac, Wolfgang Brandt, Lynne Armitage, Laura B. Sheard, Xu Tan, Geraint Parry, Haibin Mao, Ning Zheng, Richard Napier, Stefan Kepinski, Mark Estelle*

**Corresponding author. E-mail: mestelle@ucsd.edu*

SUPPLEMENTARY INFORMATION

Supplementary Methods

Supplementary Results

Supplementary Figure 1. Assembly of TIR1-IAA17, -IAA3, -IAA9, -IAA28 and -IAA31 co-receptor complexes.

Supplementary Figure 2. Sensorgram for the kinetics of TIR1- IAA7 DII association and dissociation at various concentrations of IAA.

Supplementary Figure 3. TIR1 architecture is essential for SCF^{TIR1} assembly and auxin dependent TIR1-Aux/IAA interactions.

Supplementary Figure 4. Comparison of TIR1 and AFB5 -containing auxin co-receptor complexes.

Supplementary Figure 5. Ramachandran and energy plots of the TIR1 structure 9pdb 2P1Q_B and the AFB5 structural model.

Supplementary Figure 6. AFB5 Alignment and IAA, picloram docking calculations.

Supplementary Figure 7. Differential interaction between TIR1/AFB1, 2, 5, and Aux/IAAs is unlikely to be dependent upon fusion protein expression level in yeast.

Supplementary Methods

Plant Growth Assays. Seeds were plated onto media containing ½ MS media, 1% sucrose, 1% agar, and stratified for 2-4 days before growth at 22 °C under continuous light at 110 μmol $m^{-2}s^{-1}$. For auxin growth assays, 5-day-old seedlings were transferred onto fresh MS media with or without auxin for an additional 4 days, after which the root length upon transfer was measured. Root elongation is expressed as a percentage of growth of the equivalent genotype on media without auxin. Mutant alleles have been previously described: *tir1*–1[37], *afb2–3* and *tir1-1 afb2*-3[24].

LexA yeast two hybrid assays. AFB1 (AT4G03190), AFB2 (AT3G26810), AFB3 (AT1G12820) and AFB5 (AT5G49980) cDNAs were amplified and cloned as *EcoR1* fragments in pDBD GILDA vector. Also, prey constructs were generated by cloning IAA3 (AT1G04240), IAA5 (AT1G15580), IAA7 (AT3G23050), IAA8 (AT2G22670), IAA12 (AT1G04550), IAA20 (AT2G46990), IAA28 (AT5G25890), IAA29 (AT4G32280), IAA31 (AT3G17600), ASK1 (AT1G75950) cDNAs as *EcoR1* fragments in pB42AD vector. DBD and AD constructs were transformed in either EGY48 (MATα) + *LacZ* reporter plasmid pSH18-34 or YM4271 (MATa), respectively. After mating, diploids were selected in SD-Ura-His-Trp and further streaked on Gal/Raff -Ura-His-Trp + X-Gal ± auxins for expression of the β-galactosidase reporter gene. Quantitative *LacZ* reporter activity confirmed β-galactosidase expression on plate and was measured by standard fluorescence ONPG *LacZ* assay method.

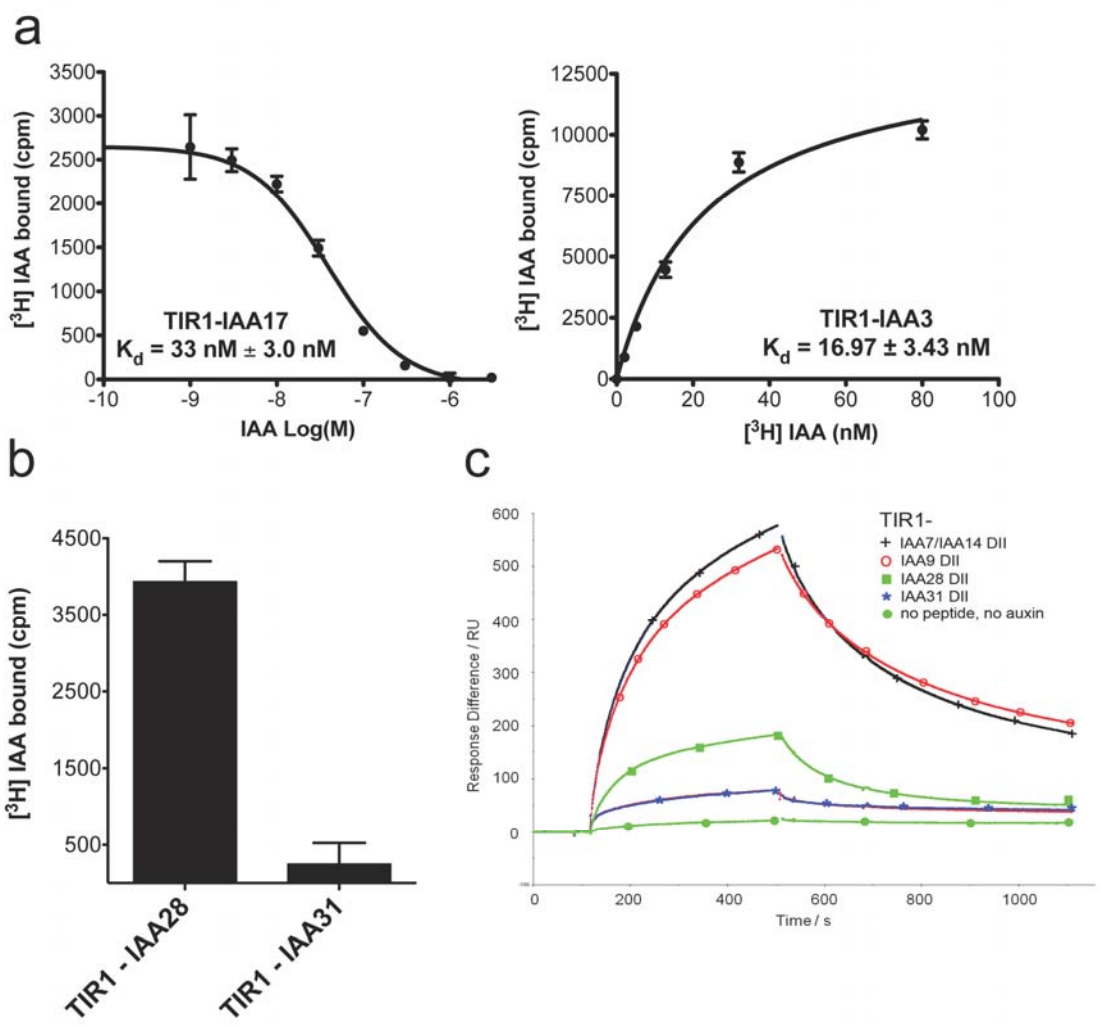

Supplementary Figure 1. Assembly of TIR1-IAA17, -IAA3, -IAA9, -IAA28 and -IAA31 co-receptor complexes. **a.** View of the TIR1-auxin binding pocket. TIR1 (grey mesh) together with the degron of IAA7 (IAA7 DII) (surface representation in yellow) equally contribute to IAA (green and red sphere) binding. **b.** Homologous binding competition assay for TIR1-IAA17 (links) and saturation binding assay for TIR1-IAA3 (right) co-receptor pairs. **b.** Binding of 200 nM [^{3}H] IAA to TIR-IAA28 and TIR1-IAA31 co-receptor complexes. TIR1-IAA31 is a low binding affinity sensor of auxin. **c.** Sensorgram showing the effect of IAA on various TIR1- Aux/IAA DII co-receptor pairs. SPR experiments were carried using SA chips with immobilized biotinylated peptides corresponding to degron (DII) of IAA7/14 (black cross), IAA9 (open red circle), IAA28 (green square) and IAA31 (blue star). TIR1 was incubated with 500 µM IAA and injected to the chips at a flow rate of 25 µL/min. Experiments were performed using a Biacore 2000.

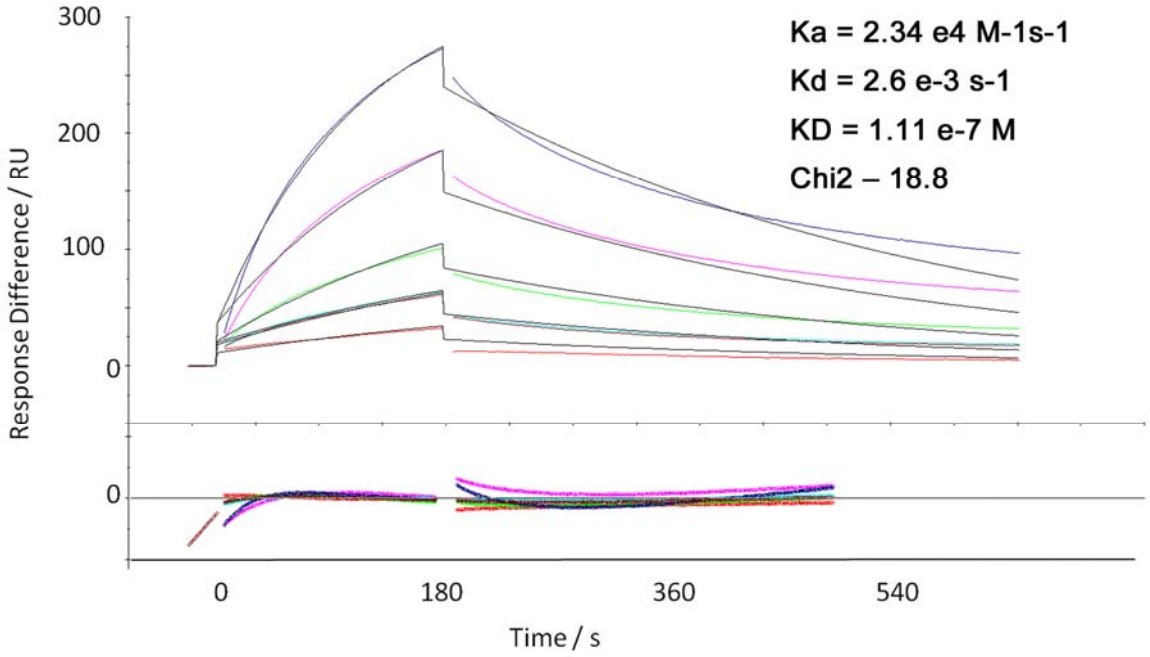

Supplementary Figure 2. Sensorgram for the kinetics of TIR1- IAA7 DII association and dissociation at various concentrations of IAA. Flow rate 25 µL/min. A Langmuir 1:1 model was used. The plot shows the dose data and the lower panel the residuals after model fitting.

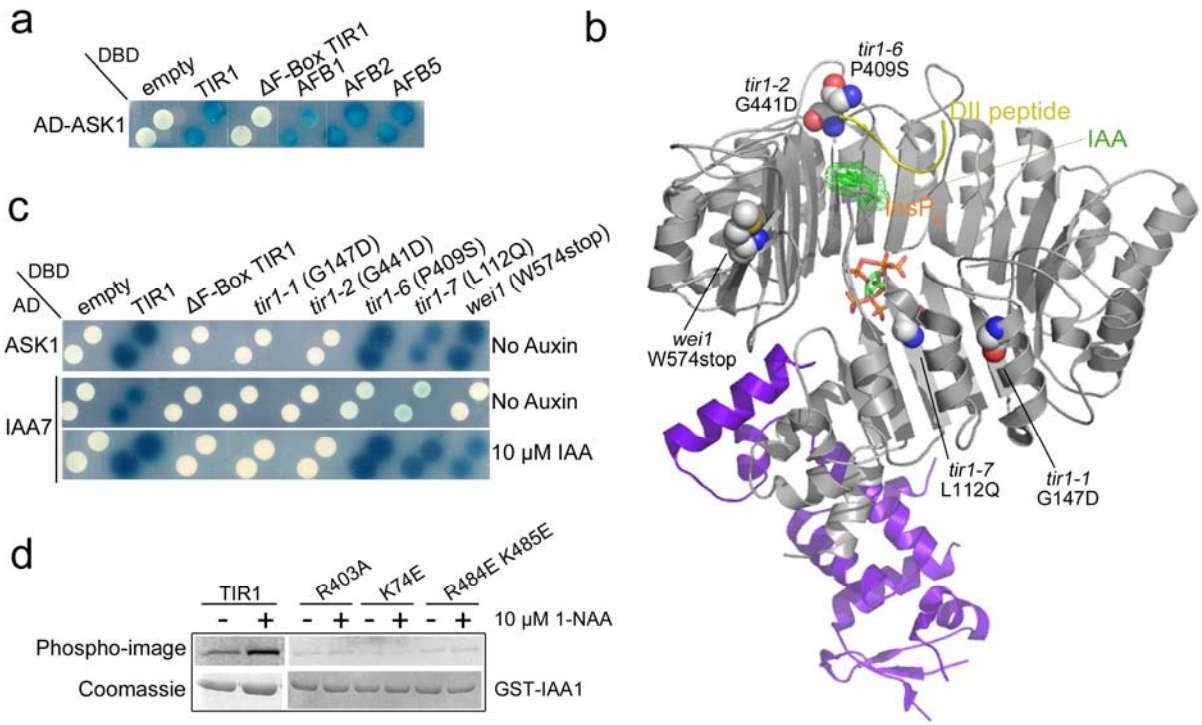

Supplementary Figure 3. TIR1 architecture is essential for SCF^{TIR1} assembly and auxin-dependent TIR1-Aux/IAA interactions. **a.** AFB1, AFB2 and AFB5 interact with ASK1 as TIR1 in yeast, suggesting that they assemble in an SCF complex. **b.** Known mutations within the LRR domain may affect TIR1 fold and compromise TIR1-ligand interactions. Ribbon view of TIR1 (grey) and ASK1 (lila). Mutant alleles that result in amino acid exchanges in the LRR Domain of TIR1 are shown as spheres. **c.** Asp to Gly amino acid exchanges in *tir1-1* and *tir1-2* mutant alleles abolish TIR1-ASK1, as well as TIR1-IAA7 interaction in yeast. *tir1-6*, *tir1-7* and *wei1* mutations seem to affect partially TIR1 function. **d.** Mutations on TIR1-auxin or -InsP6 binding sites abolished auxin dependent TIR1-IAA1 interaction in pull down assays. Experiments were carried out as described in Parry et al. 2009.

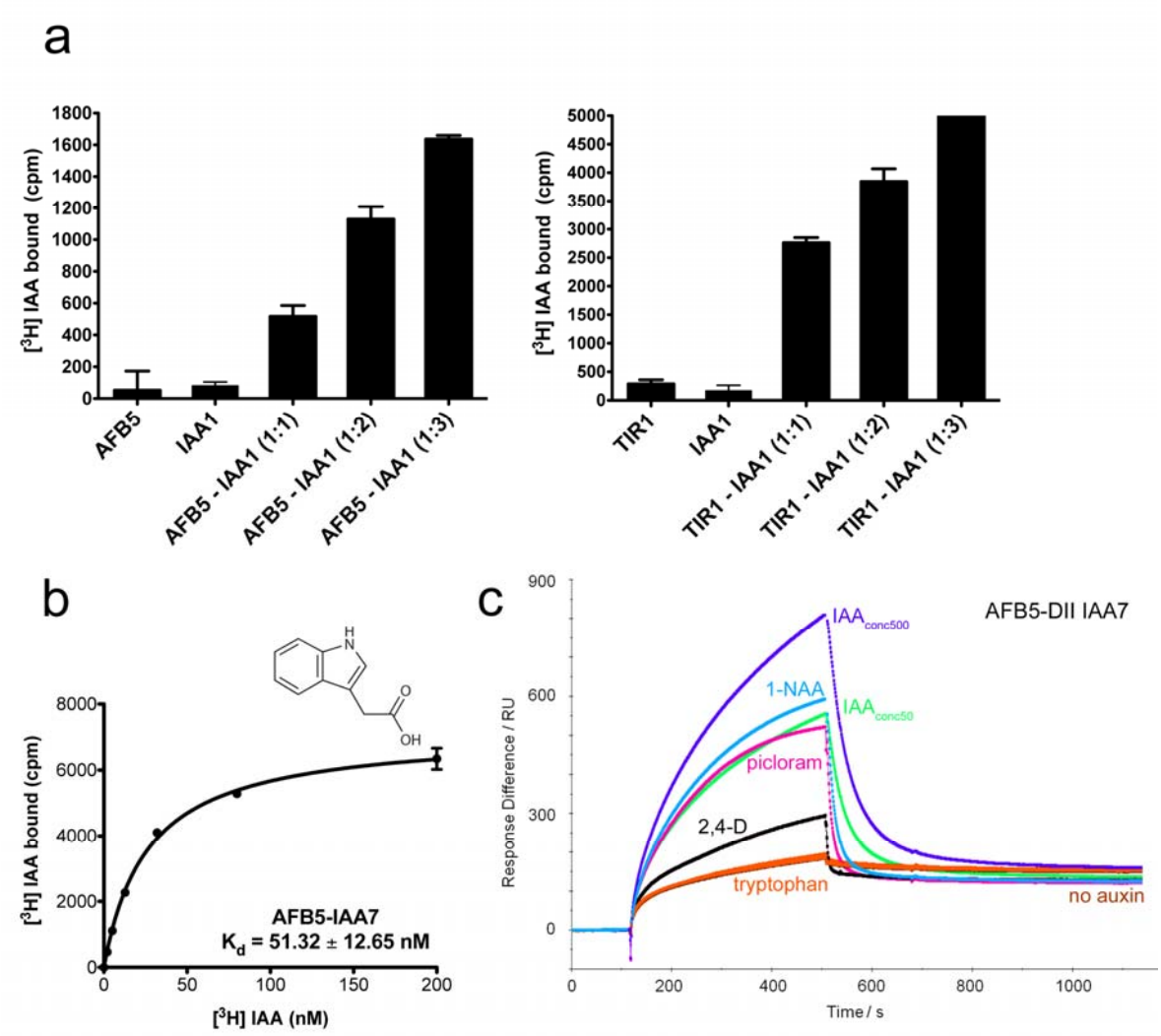

Supplementary Figure 4. Comparison of TIR1 and AFB5 -containing auxin co-receptor complexes. **a.** Auxin binding assays of TIR1-IAA1 versus AFB5-IAA1 co-receptor complexes. AFB5-IAA1 forms an auxin co-receptor comparable to TIR1-IAA1. 0.5 µg of ASK1-TIR1 or ASK1-AFB5 complexes were incubated with 1:1, 1:2 or 1:3 molar excess of GST-tagged IAA1 protein in the presence of 200 nM [^{3}H] IAA, with 1000X excess of cold IAA. **b.** Saturation binding assay shows that AFB5-IAA7 co-receptor complex exhibits a high IAA binding affinity. Assay was performed as described in Materials and Methods. **c.** SPR analysis of auxin-dependent AFB5-IAA7 DII interaction. Sensorgram shows the effect of no auxin (brown) and various auxinic compounds (500 µM IAA (blue), 50 µM IAA (light green), 50 µM 1-NAA (light blue), 50 µM 2,4-D (black), 50 µM picloram (pink), 50 µM tryptophan (orange)) on AFB5-DII peptide association and dissociation. Auxins were mixed with AFB5 in solution prior to injection over DII peptide. AFB5-IAA7 DII interaction is largely influenced by rapid off rates, in contrast to TIR1-IAA7 DII kinetic (see Figure 5b). Also, compared to TIR1-IAA7 DII, AFB5- IAA7 DII co-receptor complex exhibits a marked picloram selectivity.

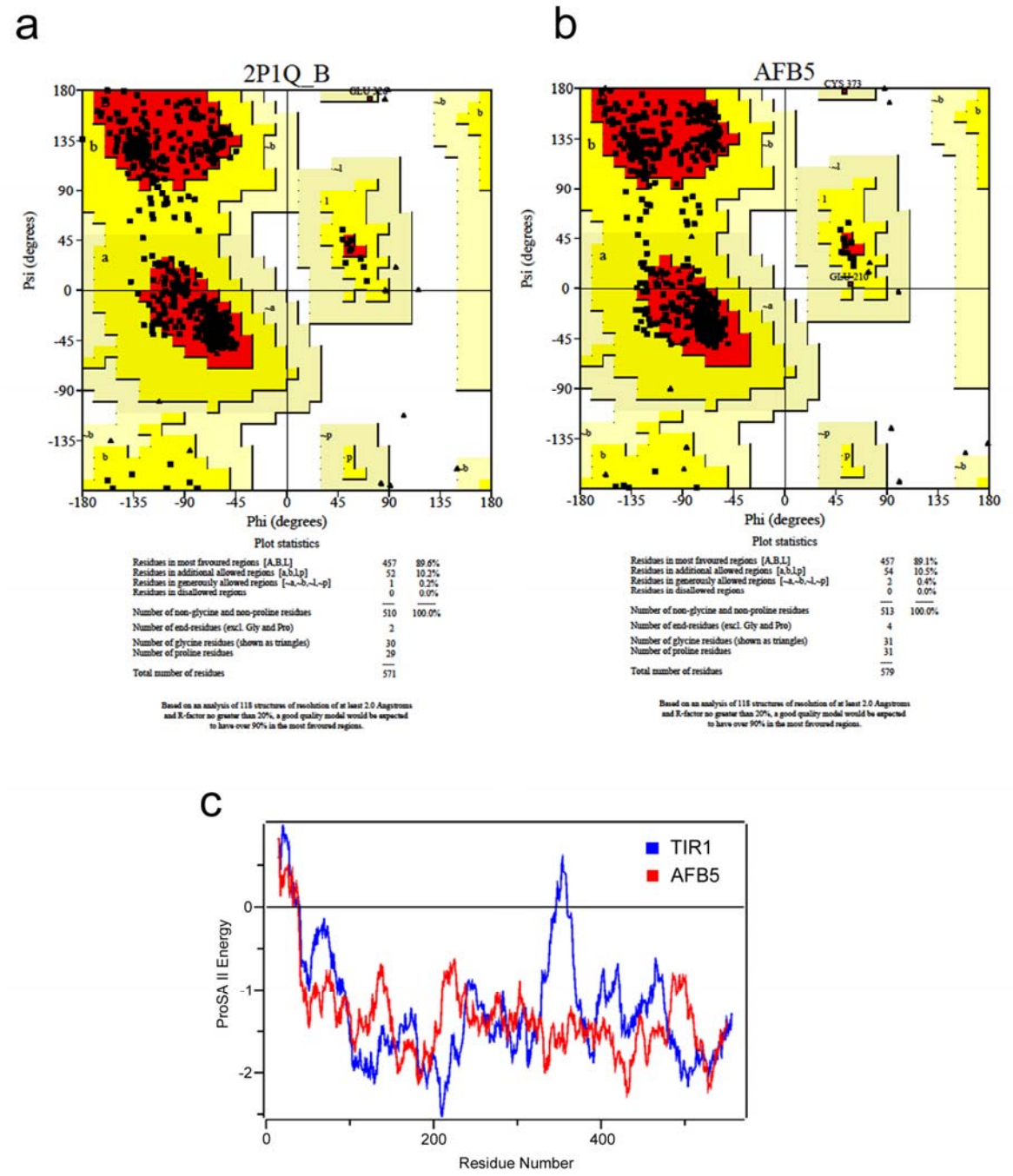

Supplementary Figure 5. a. Ramachandran plots of the TIR1 structure 9pdb 2P1Q_B) and **b.** of the AFB5 structural model. **c.** Plot of the ProSA II energy of TIR1 and AFB5 structural model. X-axis corresponds to the amino acid position and Y-axis represents a virtual energy corresponding to the overall z-score and the statistical potential of ProSA II.

a

b

	PLANTS scores		GLIDE scores (kcal/mol)	
	IAA	**picloram**	**IAA**	**picloram**
TIR1	-84.7	-72.0	-6.27	-5.82
AFB5	-90.9	-84.0	-6.91	-9.20

Supplementary Figure 6. AFB5 Alignment and IAA, picloram docking calculations. AFB5-TIR1 pairwise sequence alignment (generated by Prime, version 2.1). The sequence in pink was considered for homology modeling. Since TIR1 lacks an N-terminal extension that AFB5 possess, this fragment could not be modeled. To generate the homology model of AFB5, the following values of sequence alignment for AFB5-TIR1 were used: 46% identical, 77% similar. Fitch matrix was used to calculate similarity between TIR1 and AFB5. **b**. Scores of PLANTS and GLIDE docking (see **Material and Methods**) of IAA and picloram in TIR1 and AFB5. The negative the score, the higher the affinity for the ligand.

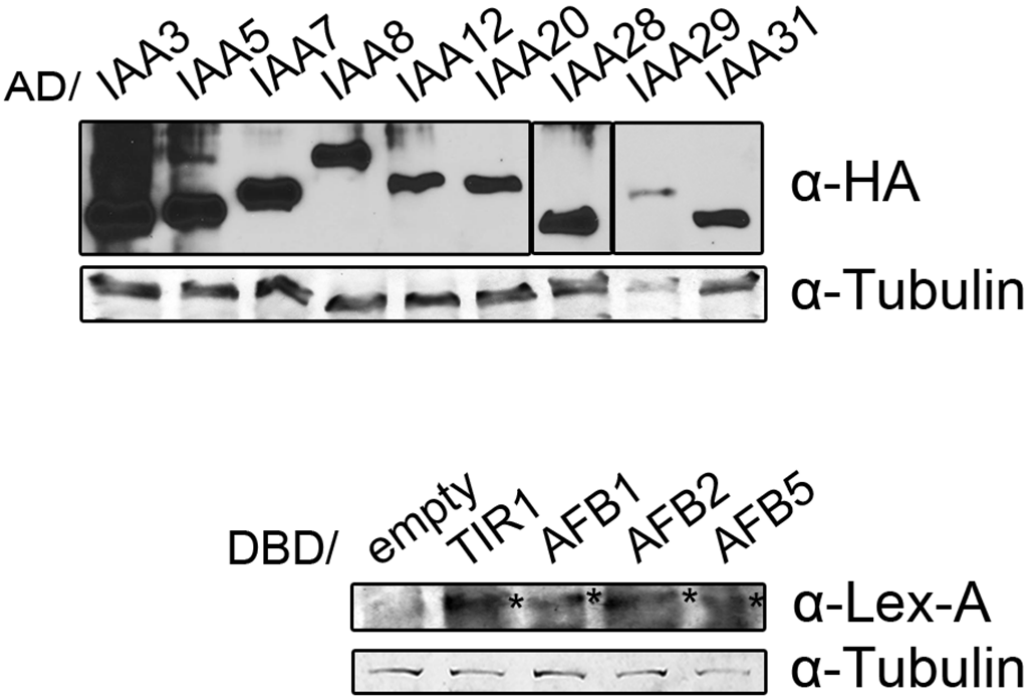

Supplementary Figure 7. Differential interaction between TIR1/AFB1, 2, 5, and Aux/IAAs is unlikely to be dependent upon fusion protein expression level in yeast. TIR1/AFB1,2,5, as well as Aux/IAA fusion proteins screened for auxin dependent interactions in yeast are well expressed. Immunoblots of HA tagged-IAA3,5,7,8,12,20,28,29 and 31 (upper panel) and LexA-fused TIR1/AFB1,2,5 (lower panel) proteins expressed under the control of the GAL1 inducible promoter an used in yeast two hybrid experiments. Total proteins were extracted from yeast diploids grown on Gal/Raff –Ura-His-Trp and detected using either anti-HA or anti-LexA antibodies. Yeast tubulin was detected with anti-tubulin antibody and used as loading control.